Am J Transl Res 2021;13(10):11235-11244
www.ajtr.org /ISSN:1943-8141/AJTR0126632

Original Article

Multi-slice CT findings in COVID-19 pneumonia: a cross-sectional multicenter study

Melike Ruşen Metin[1], Melahat Bekir Külah[2], Faruk Atabey[3], Hasan Aydin[4]

Departments of [1]Radiology, [2]Chest Diseases, [3]Radiology, University of Medipol Bahçelievler, Adnan Menderes Blv. No. 31 D: 33, 34893 Pendik, İstanbul, Turkey; [4]Department of Radiology, Ankara Oncology Research Hospital Radiology Department, Demetevler, Yenimahalle, Ankara, Turkey

Received November 19, 2020; Accepted August 3, 2021; Epub October 15, 2021; Published October 30, 2021

Abstract: In this cross-sectional study of 278 patients, patients diagnosed with COVID-19 per their clinical features, laboratory, and thorax computed tomography (CT) findings were evaluated in terms of the most common characteristic findings. The lesions were classified according to the disease stage. The most common findings for each phase were investigated. The typical CT results included ground-glass opacity (GGO), unilateral involvement, and single lesions in the early stages, as well as bilateral involvement, and multiple lesions in the progressive and peak phases. Additionally, vascular dilatation was the most common finding after GGO. Basal segment dominance and peripheral-intraparenchymal-basal segment involvement were mostly seen in the peak-phase patients. Thus, we think that this finding is an essential key to determining that the disease is in the advanced stages. The crazy-paving pattern was also a typical finding in the early-stage patients. Cavitary lesions, pulmonary nodules, and mediastinal lymph nodes were not observed in the lungs.

Keywords: SARS coronavirus, pneumonia, clinical practice guidelines, real-time PCR

Introduction

The coronavirus disease (COVID-19) broke out in Wuhan, the capital of the Hubei province of China, in December 2019. On February 11, 2020, the World Health Organization (WHO) first classified it as a coronavirus disease [1]. This ailment is an infectious condition known as severe acute respiratory syndrome and is caused by a new coronavirus. While the infection rates were decreased in China, the virus had spread rapidly to various countries worldwide, despite many efforts to limit its spread [2, 3].

In the diagnosis of COVID-19, real-time reverse-transcription polymerase chain reaction (RT-PCR) is considered as the reference standard. However, recent studies have addressed the significance of thorax computed tomography (CT) examinations in COVID-19 patients with false-negative RT-PCR results and have reported CT sensitivities as high as 98% [4, 5]. The RT-PCR test should be repeated in patients who have positive CT findings and a high clinical suspicion but with a negative RT-PCR analysis [6].

In most patients with COVID-19, there are characteristic CT findings which are detected from the onset of the symptoms that determine the diagnosis and treatment [7, 8]. The most prominent CT finding defined in the literature is ground-glass densities which are located posteriorly in the bilateral peripheral areas [8-10]. However, recent CT findings such as crazy-paving, reverse halo signs, pulmonary nodule, vascular and bronchial dilatations, and air bubble signs have been described [4-7, 9, 10].

This study aimed to evaluate the multi-detector CT (MDCT) findings of the patients who were referred to our hospital with suspected COVID-19 infections, to evaluate the CT findings of the patients who were treated without intensive care, and to investigate the frequency of elementary lesions.

Methods

This retrospective study was approved by our local ethics committee, with ethical approval number E-19-114. Recent coronavirus publications related to COVID-19 were all examined

Table 1. A descriptive presentation of the participants' basic clinical features

		n	%
Stage	Ultra-early phase	20	10.2
	Early phase	79	40.3
	Progressive phase	81	41.3
	Peak phase	16	8.1
Affected side	Bilateral	145	74.0
	Unilateral	51	26.0
Multilobar disease	Lobar disease	46	23.5
	Multilobar	137	69.9
	Bilobar	13	6.6
Number of lesions	Multiple lesions	166	84.7
	Single lesion	30	15.3

for this paper. Clinical findings, as well as epidemiological information, laboratory results, and imaging findings of 278 suspected COVID-19 cases between 11.03.2020 and 22.04. 2020 were evaluated retrospectively in our group of hospitals (Medipol Mega University Hospital, Istanbul Medipol University Pendik Education and Research Hospital, Koşuyolu Istanbul Medipol Hospital and Çamlıca Medipol University Hospital).

Assessment of the CT images

The image analysis and MDCT scoring were performed by two radiologists with 20-22 years of experience. The CT images were investigated for each patient and were evaluated in the coronal, sagittal, and axial planes by performing multiplanar reconstruction (MPR).

With regard to the literature, thorax CT findings such as ground-glass opacity (GGO), crazy-paving, consolidation, cavitation, air bronchograms, air bubbles, pulmonary nodules, pleural shrinkage, pleural thickening, fibrotic tape, vascular dilatation, bronchial deformity, the presence of mediastinal lymph nodes, reverse halo appearance, localization of the lesions, and the affected lung lobes were recorded for each patient. Lymph nodes smaller than 10 mm in diameter were not evaluated when mediastinal lymph nodes were assessed. The stage of the disease at the time of diagnosis (ultra-early, early, progression, peak, and absorption phases) was determined according to the clinical and CT findings [10, 11].

Technical features of the MDCT: Low-dose CT techniques were used for the MDCT. CT examinations were performed from the lung apexes to the costophrenic angles using the following tomography devices while the patient was in a supine position while holding his/her breath:

1- Multi-slice (128 slices) Siemens Healthineers SOMATOM go. ALL Device: Study parameters: tube voltage 80-120 kV, tube current 10-25 mAs or intelligent mAs, pitch 0.60 mm, FOV: 350-400 mm, slice thickness 1.5 mm.

2- Multi-slice (16-32 with IVR) Siemens SOMATOM Go. Now Device. Study parameters: tube voltage: 80-130 kV, tube current 9-900 mAs, pitch 0.35, FOV: 350-400 mm, slice thickness 5 mm.

Statistical methods

The data were analyzed using Statistical Package for the Social Sciences (SPSS) version 25.0 (SPSS Inc., Chicago, IL, USA). The results are presented as frequencies, percentages, means, and standard deviations (SD). Chi-square tests (or Fisher's exact tests) were used to check the differences between the variables. For the Fisher's exact tests, each subscript letter denotes a subset of the stage categories whose column proportions do not differ significantly from each other at the 0.05 level (corrected using Bonferroni corrections). The significant differences between the multiple subgroup comparisons were presented after we made the Bonferroni corrections.

A *P*-value of <0.05 was considered statistically significant.

Results

Participants

The data from the 196 patients were analyzed. 60.7% (n=119) of the participants were men and 39.3% (n=77) were women. The mean age of the participants was 47.74±14.68 years. The vast majority of the patients (99.0%, n=194) were between 20-80 years of age. There was only one patient (0.5%) who was 5 years old, and another one (0.5%) who was 91 years old.

Descriptive findings

Most patients were classified as being in the early or progressive phases, with bilateral involvement and multilobar disease with multiple lesions (**Table 1**).

Table 2. The descriptive radiological findings

	No		Yes	
	n	%	n	%
Ground-glass appearance and consolidation	149	76.0	47	24.0
Pleural retraction	74	37.8	122	62.2
Pleural effusion	188	95.9	8	4.1
Pleural thickening	135	68.9	61	31.1
Lymph node	196	100.0	0	0.0
Ground-glass appearance	7	3.6	189	96.4
Presence of air bubble	155	79.1	41	20.9
Air bronchogram	164	83.7	32	16.3
Reverse halo	171	87.2	25	12.8
Vascular enlargement sign	14	7.1	182	92.9
Pulmonary nodule	158	80.6	38	19.4
Crazy paving	85	43.4	111	56.6
Fibrotic bands	171	87.2	25	12.8
Basal segment dominance	172	87.8	24	12.2
Bronchial deformation sign	167	85.2	29	14.8

Radiographically, the most prominent feature was the ground-glass appearance (GGO) (present in 96.4% of the cases). However, the presence of the vascular enlargement sign was the second common finding, and it was encountered in 92.9% of the patients (**Table 2**). None of the patients had positive lymph nodes radiologically.

Clinical findings: A total of 82 patients, including patients with negative RT-PCR tests, were excluded, including the patients in the intensive care unit, patients who were clinically and radiologically in the absorption phase, and patients with concomitant diseases (such as a history of tuberculosis, masses in the lungs or the mediastinum, and chronic interstitial lung diseases). The body weights of the patients varied between 40 and 110 kg, with 75 kg the average.

The diagnoses of the 196 patients were confirmed with respect to their clinical findings, laboratory tests, and thorax CTies. Some of the patients included in the study had a negative initial RT-PCR analysis, followed by a positive second or third PCR test. All the patients were outpatients without any severe symptoms. Inpatients, intensive care patients, and intubated patients were not included in the study cohort. Most of the patients had a fever, a cough, a loss of smell and taste, and sore-throat like symptoms, and some of them had a filiation and touch history without any symptoms.

Laboratory findings: Among the main routine tests requested for the patient group, we examined complete blood count (CBC), D-dimer, C-reactive protein (CRP), ferritin, lactate dehydrogenase (LDH), alanine aminotransferase (ALT) and aspartate aminotransferase (AST). Lymphopenia accompanied by mild thrombocytopenia was the most prominent finding in the majority of the participants (50.8%). The occurrence of coagulopathy and high D-dimer levels, which indicated a progression of the disease, was observed in 34.24% of our patients. The CRP values were used to show the progression of the disease, and they were high in 75.9% of our patient group. High ferritin values were also found in 87.8% of the patients, similar to the CRP values. LDH, which is an important marker for lung damage, was high in 55.1% of our patients. In addition, ALT (21%) and AST (22.6%) were found to be high in some patients.

Outcomes

The clinical and radiological findings were compared with the disease stages. For the statistical comparison, the ultra-early and early phases were combined. The analysis which demonstrated significant differences between the different stages of the disease were concerned with most of the examined clinical and radiological variables (**Table 3**). One interesting finding was that the GGO and the consolidations increased as the disease progressed, but there was no significant difference between the GGO and the disease stage. However, only 3.6% (n=7) of the participants lacked a ground-glass picture.

The ultra-early & early phases, the progressive phase, and the peak phase distributions of the stages of the disease between males and females were 55.6% (n=65) vs. 45.3% (n=34), 40.2% (n=47) vs. 45.3% (n=34), and 4.3% (n=5) vs. 9.3% (n=7), respectively. There were no significant differences between the males and

Table 3. A comparison of the clinical and radiological findings and the disease stage

		Stage						X^2	p
		Ultra-early & early phase		Progressive phase		Peak phase			
		n	%	n	%	n	%		
Affected side	Bilateral	60[a]	42.6	69[b]	48.9	12[b]	8.5	18.427	<0.001
	Unilateral	39[a]	76.5	12[b]	23.5	0[b]	0.0		
Affected lobes	Lobar	36[a]	78.3	10[b]	21.7	0[b]	0.0	20.342*	<0.001
	Multilobar	55[a]	41.4	66[b]	49.6	12[b]	9.0		
	Bilobar	8[a]	61.5	5[a]	38.5	0[a]	0.0		
Ground-glass appearance and consolidation	No	97[a]	66.4	48[b]	32.9	1[c]	0.7	68.872	<0.001
	Yes	2[a]	4.3	33[b]	71.7	11[c]	23.9		
Ground-glass appearance	No	3[a]	42.9	4[a]	57.1	0[a]	0.0	0.563*	0.812
	Yes	96[a]	51.9	77[a]	41.6	12[a]	6.5		
Pleural retraction	No	57[a]	77.0	15[b]	20.3	2[b]	2.7	31.276	<0.001
	Yes	42[a]	35.6	66[b]	55.9	10[b]	8.5		
Pleural effusion	No	98[a]	53.3	77[a]	41.8	9[b]	4.9	10.537*	0.003
	Yes	1[a]	12.5	4[a]	50.0	3[b]	37.5		
Pleural thickening	No	84[a]	63.2	40[b]	30.1	9[b]	6.8	26.522	<0.001
	Yes	15[a]	25.4	41[b]	69.5	3[b]	5.1		
Number of lesions	Multiple	73[a]	45.1	77[b]	47.5	12[b]	7.4	17.737	<0.001
	Single	26[a]	86.7	4[b]	13.3	0[b]	0.0		
Presence of air bubble	No	89[a]	58.6	58[b]	38.2	5[b]	3.3	19.954	<0.001
	Yes	10[a]	25.0	23[b]	57.5	7[b]	17.5		
Air bronchogram	No	97[a]	60.2	61[b]	37.9	3[c]	1.9	49.660	<0.001
	Yes	2[a]	6.5	20[b]	64.5	9[c]	29.0		
Reverse halo	No	92[a]	54.8	65[b]	38.7	11[b]	6.5	6.755	0.033
	Yes	7[a]	29.2	16[b]	66.7	1[b]	4.2		
Vascular enlargement sign	No	6[a]	42.9	7[a]	50.0	1[a]	7.1	0.460	0.831
	Yes	93[a]	52.2	74[a]	41.6	11[a]	6.2		
Pulmonary nodule	No	75[a]	48.4	69[a]	44.5	11[a]	7.1	3.529	0.171
	Yes	24[a]	64.9	12[a]	32.4	1[a]	2.7		
Crazy paving	No	58[a]	69.0	23[b]	27.4	3[b]	3.6	18.329	<0.001
	Yes	41[a]	38.0	58[b]	53.7	9[b]	8.3		
Fibrotic bands	No	98[a]	57.6	63[b]	37.1	9[b]	5.3	22.072	<0.001
	Yes	1[a]	4.5	18[b]	81.8	3[b]	13.6		
Basal segment dominance	No	99[a]	58.2	65[b]	38.2	6[b]	3.5	35.875	<0.001
	Yes	0[a]	0.0	16[b]	72.7	6[b]	27.3		
Bronchial deformation sign	No	93[a]	56.7	63[a]	38.4	8[b]	4.9	12.954	0.003
	Yes	6[a]	21.4	18[a]	64.3	4[b]	14.3		
Basal-peripheral-intraparenchymal disease	PD	50[a]	75.8	15[b]	22.7	1[b]	1.5	51.625*	<0.001
	PID	48[a]	44.0	58[b]	53.2	3[a]	2.8		
	B-PID	1[a]	5.9	8[b]	47.1	8[c]	47.1		

*Fisher's exact test, PD: Peripheral disease, PID: Peripheral-intraparenchymal disease, B-PID: Basal-peripheral-intraparenchymal disease. [a,b,c]: Each subscript letter denotes a subset of stage categories whose column proportions do not differ significantly from each other at the 0.05 level (corrected after Bonferroni).

females in terms of the disease stages (chi-square =3.087, P=0.214). However, the mean age was increasingly parallel to the disease stage. The mean ± standard deviations of age

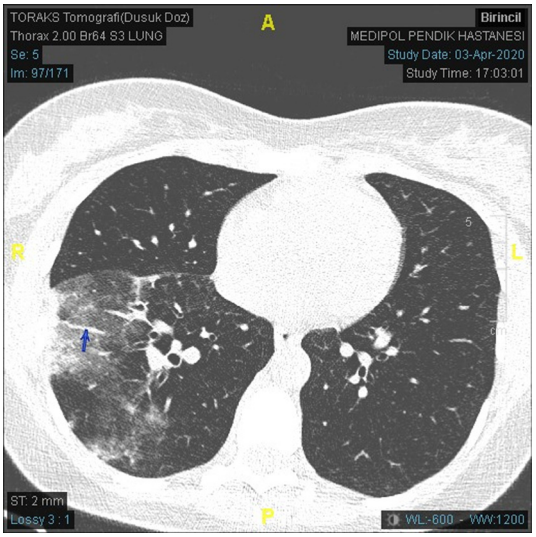

Figure 1. Ground glass density, subpleural consolidation, and vascular dilatation (arrow) in the right lung lower lobe anterior segment.

among the patients in the ultra-early & early phases, the progressive phase, and the peak phase were 43.94±13.24, 50.68±15.08, 58.42±13.69, and 47.69±14.64 years, respectively (one-way ANOVA F=8.823, P<0.001).

Discussion

Coronavirus is an enveloped RNA virus that causes acute respiratory infections in humans. Due to its ability to infect multiple hosts and cause different diseases, this virus is considered a complex pathogen [11, 12]. Except for older people (>70 years) with COVID-19 infection comorbidity, it has a relatively low mortality rate (3-5%) [12, 13]. It is estimated that 15-20% of infected people develop severe pneumonia, and 5-10% require critical care [11-13].

RT-PCR tests requires rigorous laboratory work, and it takes a long time to get the results. Also, in some patients with suspected COVID-19, the RT-PCR may generate a false-negative result. Especially considering the limited use of the RT-PCR test and its false-negative rate, routine unenhanced thorax CT exams are a useful option for the early detection of COVID-19 infections [10-14].

Since 13.02.2020, several articles about the imaging features of COVID-19 have been published in radiology journals [9, 14-17]. In the 6th version of the diagnosis and treatment protocol on 18.02.2020, the diagnosis of viral pneumonia based on radiological features was established as one of the diagnostic criteria [18].

Studies on CT findings in the diagnosis and the treatment of COVID-19 are still scarce, indicating the need for further studies. Thorax CT images may appear within different imaging patterns that vary with the period and severity of the disease [7, 19]. Recent studies have shown that the CT properties of COVID-19 are related to the duration of the infection and can be divided into four stages: the early phase, the progressive phase, the peak phase, and the absorption phase, based on their CT results: (1) the early stage (0-4 days) that shows small GGO distributed subpleurally in the lower part, (2) the progressive stage (5-8 days) with the infection quickly extended and widened to the bilateral multilobes with diffusely scattering GGO, consolidation, and the crazy-paving pattern, (3) the peak stage (10-13 days) that shows the slow expansion of the involved part to the peak involvement, including diffuse GGO, a crazy-paving pattern, residual parenchymal bands, and consolidation, and finally the absorption stage (14-27 days) which predicts the recovery of all the lung parenchymal findings mainly with fibrosis and/or fibrotic bands [8, 11, 20]

We compared the thorax CT findings of 196 patients diagnosed using PCR tests with clinical clues by categorizing the patients into three groups, namely, the ultra-early phase, the early phase, the progressive phase, and the peak phase (the patients in the absorption phase were excluded). However, to enable the analysis, the ultra-early and early stages were combined.

GGO, an elementary lesion, has been described as the earliest finding in some articles [9] (**Figure 1**). In our study, no significant difference was found between the stage of the disease and the frequency of GGO, and only 3.6% of the patients had no GGO. Our results were consistent with the literature suggesting that the most common (96.4%) imaging finding with a rate up to 98% was GGO [21, 22]. According to the biopsy results published by Xu Zhe on 17.02.2020, pulmonary edema and hyaline membrane formation in both lungs might

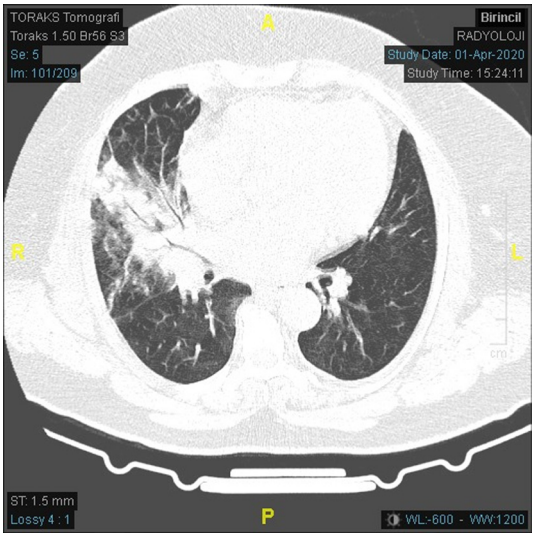

Figure 2. Ground glass density and consolidation seen together.

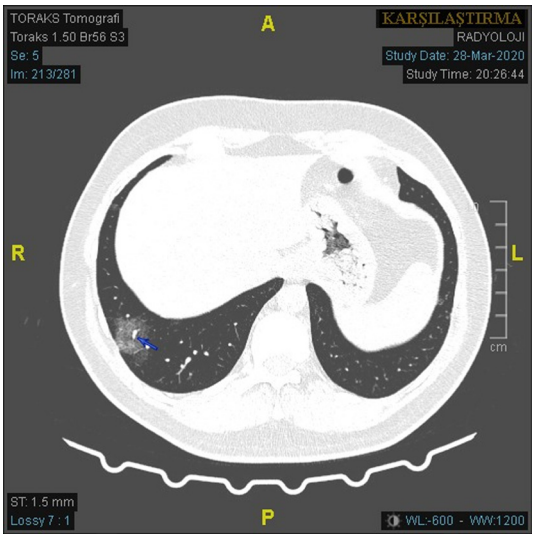

Figure 3. Remarkable ground-glass density and vascular dilatation in the lower right lower lobe in the axial sections.

explain the pathological process that results in the GGO finding [23].

One of the remarkable findings in our series was that the consolidation was mostly accompanied by GGO (68.8%) (**Figure 2**). In our patients, GGO was seen in the periphery of the consolidated segment-subsegment or in another localization. However, the number of patients with consolidation was significantly lower than the number of patients with GGO ($P<0.001$). Parallel to our results, in several

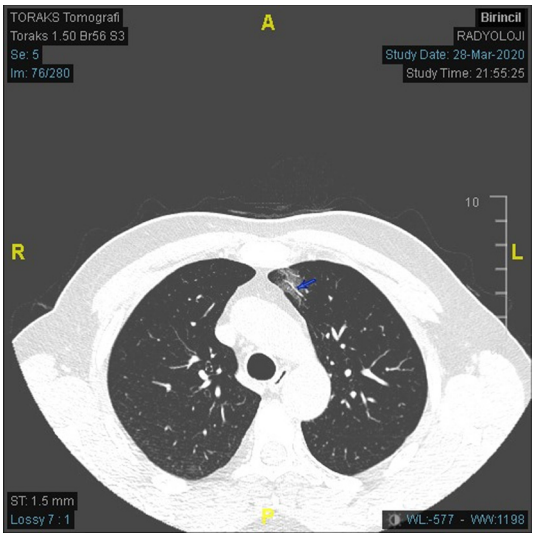

Figure 4. Pathological peripheral ground-glass densities in the left lung and signs of vascular dilatation (arrow).

recent studies, it was concluded that GGO can progress or coexist within 1-3 weeks [7, 19]. Li did not detect a consolidation in any patient without GGO [24].

The vascular dilatation sign was the dilated pulmonary vessels, which were observed around or inside the lesions in the CT (**Figures 3**, **4**). The most remarkable and probably omitted finding in our study was the vascular dilatation, which was found in all the phases at a high rate (92.9%). As Xu Zhe stated in the pathological examinations, this finding might be attributed to the damage and expansion of the capillary walls caused by the pro-inflammatory factors [23, 25].

Crazy-paving was seen as thickened interlobular septa and intralobular lines superimposed on the GGO background [19, 26] (**Figure 5**). This finding might result from alveolar edema and interstitial inflammation due to acute lung injury [27, 28]. In recent studies, the crazy-paving pattern was reported in 5-36% of COVID-19 patients [20, 21]. In our study, crazy-paving was observed in 38% of patients in the early-phase, 53.7% of patients in the progression-phase, and 8.3% of patients in the peak-phase.

In our study, bronchial deformation findings indicating a close relationship between the GGO and crazy paving patterns or mild bronchial dilatation and millimetric nodular irregu-

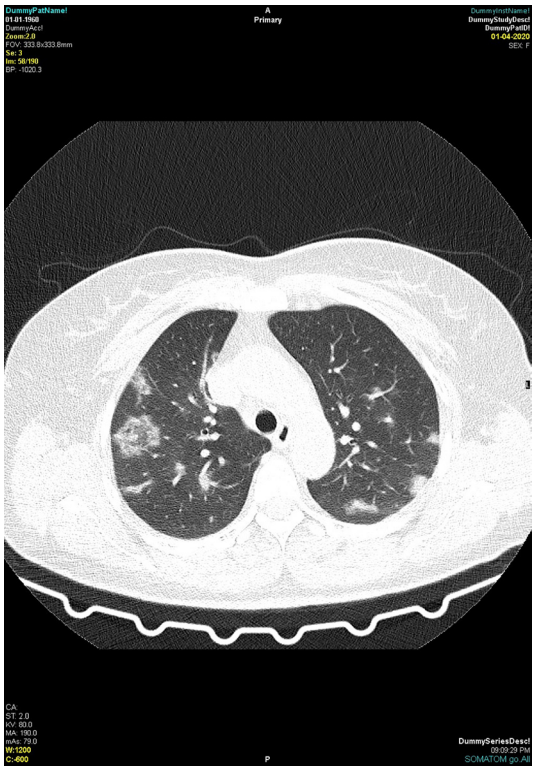

Figure 5. Ground glass density in both lungs and the crazy-paving pattern in the upper lobe of the right lung.

larities in the bronchial walls were found in 14.8% of the patients, and significantly less in the early-phase patients (**Figure 6**). In other phases, there was no significant difference in the frequency of bronchial deformations. In the literature, bronchial wall thickening has been reported in approximately 10% to 20% of COVID-19 patients, which is consistent with our study [21, 22, 27]. Li K reported that the incidence of bronchial wall thickening was significantly higher in patients with COVID-19 and in severe/critical patients compared to normal patients and is linked to the pathogenesis of this finding via the destruction of the bronchial wall structure and the proliferation of fibrous tissue [21]. Jin also described typical and atypical chest CT patterns and reported that approximately 7% of the patients had bronchial wall thickening [11].

Pulmonary nodules and halo findings describe the millimetric nodules in CT with a dense central part and GGO at the periphery. When they were evaluated in the context of the MIP images, we thought that the central dense area

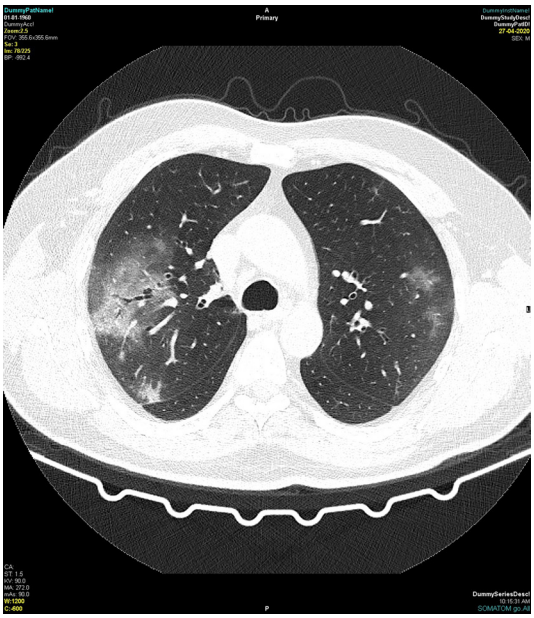

Figure 6. Ground glass density in both lungs and the crazy-paving pattern in the upper lobe of the right lung.

might be called dilated vascular structures. However, a histopathological confirmation of this finding had to be warranted. We observed this finding at the rate of 19.4%, and there was no significant difference between the phases. However, Zhou reported this finding as the single distinctly different CT finding in the early period of COVID-19 among all CT findings and stated that the halo sign rapidly transforms into GGO within a week due to the exacerbation of COVID-19 [29].

Pleural effusion, pericardial effusion, lymphadenopathy, cavitation, and pneumothorax have been reported less commonly or rarely in the literature [30-32]. None of our patients had cavitation, centrilobular nodule, pericardial effusion, pneumothorax, or lymphadenopathy. The finding of pleural retraction was significantly higher in the early phase (77%). Nevertheless, pleural effusion was seen in only one patient in the early phase, but it was significantly higher (37.5%) in the peak phase. On the other hand, effusion was observed in 4.1% of all patients. This suggests that the presence of pleural effusion indicates a poor prognosis in COVID-19. Similar to our findings, a recent study involving 81 patients with COVID-19 reported pleural effusions in only 5% of the patients [20].

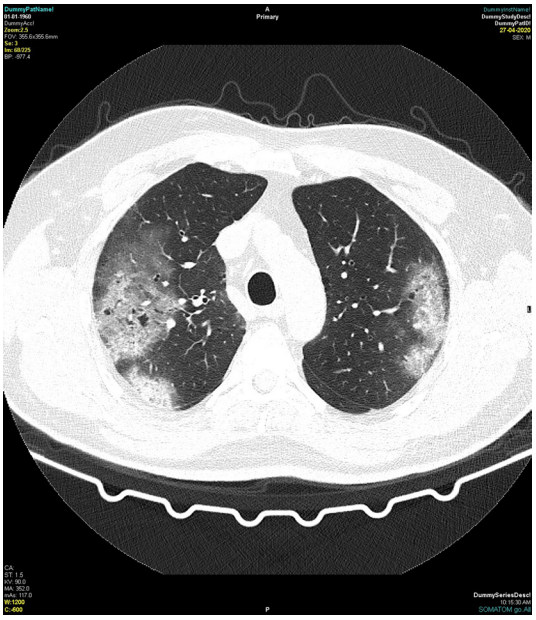

Figure 7. Bronchial deformation and minimal dilation (arrow).

In a recent prospective series with 41 patients, 98% had bilateral lung involvement [25]. Pan reported that approximately 70% of patients had multilobar involvement, consistent with other studies [33]. In our patient group, bilateral involvement was significantly higher than unilateral involvement, and the presence of multilobar disease was significantly higher than bi-lobar and lobar involvement (P<0.001). Unilateral involvement (76.5%), single lobe involvement (78.3%), and single lesion detection rates (86.7%) were significantly higher in the early phase than in the other phases (P<0.001), and no single lesion was detected in the peak phase as expected.

75.8% of our patients were early phase patients with a peripheral-subpleural disease. Patients with peripheral-intraparenchymal involvement were significantly higher in the progressive phase. There were no initial-phase patients with basal-peripheral-intraparenchymal involvement. Basal segment dominance was not seen in any patient in the early stage, but it was observed in half of the peak phase patients and 72.7% of the patients in the progression phase. Therefore, mixed type involvement and basal segment dominance might be a signal indicating that COVID-19 pneumonia is leading to a progressive or peak phase.

Air bronchogram findings were observed in only two patients in the early phase. This finding was significantly higher in the progression phase compared to the other stages. While only ten patients were found to have air bronchograms in the early phase, there were twenty-three in the progressive phase and seven in the peak phase. The frequency of air bubble findings in the early phase was significantly lower (**Figure 7**). The incidences of reverse halo findings did not differ significantly between the progression phase and the peak phase, but it was significantly lower in the early phase.

Conclusion

The number of COVID-19 cases in Turkey has been increasing daily like in many countries. Due to the high false-negative rate of RT-PCR testing, thorax CT findings are becoming increasingly important and provide clinicians with diagnostic guidance, enabling them to manage their patients effectively.

There are typical and atypical thorax CT findings that vary according to the COVID-19 pneumonia phase. Therefore, the analysis of the images obtained during the onset of the disease and its follow-up are significant. Our results are consistent with the literature presenting GGO as the most common imaging finding, with a prevalence of up to 98%. However, when compared with other studies, we detected a rate of 92.9% for the presence of vascular dilatation, a finding that was not mentioned earlier and that has not received adequate attention. We think that ongoing studies should pay more attention to vascular dilatation.

As clinical experiences have been increased and improved for the early diagnosis and treatment of COVID-19 patients, we hope that the thorax CT findings will provide more accurate information regarding the phase and the course of the disease.

Limitations

This was a retrospective study, and it might not have been possible to exclude superinfection in some patients. Additionally, the histopathological features of the lesions detected on CT could not be investigated naturally.

The CT examinations were also carried out using two different models of CT scanners.

Disclosure of conflict of interest

None.

Address correspondence to: Hasan Aydin, Department of Radiology, Ankara Oncology Research Hospital Radiology Department, Demetevler, Yenimahalle, Ankara, Turkey. Tel: +0090-5323484530; E-mail: dr.hasanaydin@hotmail.com

References

[1] Coronaviridae Study Group of the International Committee on Taxonomy of Viruses. The species severe acute respiratory syndrome-related coronavirus: classifying 2019-nCoV and naming it SARS-CoV-2. Nat Microbiol 2020; 5: 536-44.

[2] Zhu N, Zhang D, Wang W, Li X, Yang B, Song J, Zhao X, Huang B, Shi W, Lu R, Niu P, Zhan F, Ma X, Wang D, Xu W, Wu G, Gao GF and Tan W; China Novel Coronavirus Investigating and Research Team. A novel coronavirus from patients with pneumonia in China, 2019. N Engl J Med 2020; 382: 727-33.

[3] World Health Organization (WHO). Coronavirus disease (COVID-2019) situation reports. 2020.

[4] Fang Y, Zhang H, Xie J, Lin M, Ying L, Pang P and Ji W. Sensitivity of chest CT for COVID-19: comparison to RT-PCR. Radiology 2020; 296: E115-17.

[5] Yang W, Cao Q, Qin L, Wang X, Cheng Z, Pan A, Dai J, Sun Q, Zhao F, Qu J and Yan F. Clinical characteristics and imaging manifestations of the 2019 novel coronavirus disease (COVID-19): a multi-center study in Wenzhou city, Zhejiang, China. J Infect 2020; 80: 388-93.

[6] Xie X, Zhong Z, Zhao W, Zheng C, Wang F and Liu J. Chest CT for typical 2019-nCoV pneumonia: relationship to negative RTPCR testing. Radiology 2020; 200343.

[7] Shi H, Han X, Jiang N, Cao Y, Alwalid O, Gu J, Fan Y and Zheng C. Radiological findings from 81 patients with COVID-19 pneumonia in Wuhan, China: a descriptive study. Lancet Infect Dis 2020; 20: 425-34.

[8] Wang D, Hu B, Hu C, Zhu F, Liu X, Zhang J, Wang B, Xiang H, Cheng Z, Xiong Y, Zhao Y, Li Y, Wang X and Peng Z. Clinical characteristics of 138 hospitalized patients with 2019 novel coronavirus-infected pneumonia in Wuhan, China. JAMA 2020; 323: 1061-9.

[9] Chung M, Bernheim A, Mei X, Zhang N, Huang M, Zeng X, Cui J, Xu W, Yang Y, Fayad ZA, Jacobi A, Li K, Li S and Shan H. CT imaging features of 2019 novel coronavirus (2019-nCoV). Radiology 2020; 295: 202-7.

[10] Li Y and Xia L. Coronavirus Disease 2019 (COVID-19): role of chest CT in diagnosis and management. Am J Roentgenol 2020; 214: 1280-6.

[11] Jin YH, Cai L, Cheng ZS, Cheng H, Deng T, Fan Jin YH, Cai L, Cheng ZS, Cheng H, Deng T, Fan YP, Fang C, Huang D, Huang LQ, Huang Q, Han Y, Hu B, Hu F, Li BH, Li YR, Liang K, Lin LK, Luo LS, Ma J, Ma LL, Peng ZY, Pan YB, Pan ZY, Ren XQ, Sun HM, Wang Y, Wang YY, Weng H, Wei CJ, Wu DF, Xia J, Xiong Y, Xu HB, Yao XM, Yuan YF, Ye TS, Zhang XC, Zhang YW, Zhang YG, Zhang HM, Zhao Y, Zhao MJ, Zi H, Zeng XT, Wang YY and Wang XH; for the Zhongnan Hospital of Wuhan University Novel Coronavirus Management and Research Team, Evidence-Based Medicine Chapter of China International Exchange and Promotive Association for Medical and Health Care (CPAM). A rapid advice guideline for the diagnosis and treatment of 2019 novel coronavirus (2019-nCoV) infected pneumonia (standard version). Mil Med Res 2020; 7: 4.

[12] Fung TS and Liu DX. Human coronavirus: host-pathogen interaction. Annu Rev Microbiol 2019; 73: 529-57.

[13] WHO. Who Director-General's opening remarks at the media briefing on COVID-19. 2020.

[14] Novel Coronavirus Pneumonia Emergency Response Epidemiology Team, on behalf of the Chinese Centre for Disease Control and Prevention. The epidemiological characteristics of an outbreak of 2019 novel coronavirus diseases (COVID-19)-China, 2020. CCDC Weekly 2020; 2: 113-22.

[15] Lei J, Li J, Li X and Qi X. CT imaging of the 2019 novel coronavirus (2019-nCoV) pneumonia. Radiology 2020; 295: 18.

[16] Fang Y, Zhang H, Xu Y, Xie J, Pang P and Ji W. CT Manifestations of two cases of 2019 novel coronavirus (2019-nCoV) Pneumonia. Radiology 2020; 295: 208-209.

[17] Shi H, Han X and Zheng C. Evolution of CT manifestations in a patient recovered from 2019 novel coronavirus (2019-nCoV) pneumonia in Wuhan, China. Radiology 2020; 295: 20.

[18] National Health Commission of the People's Republic of China website. Diagnosis and treatment of novel coronavirus infection (trial version 6). www.nhc.gov.cn/yzygj/s7653p/202002/8334a8326dd94d329df351d7da8aefc2.shtml. Published February 18, 2020. Accessed February 19, 2020.

[19] Pan F, Ye T, Sun P, Gui S, Liang B, Li L, Zheng D, Wang J, Hesketh RL, Yang L and Zheng C. Time course of lung changes on chest CT during recovery from 2019 novel coronavirus (COV-

ID-19) pneumonia. Radiology 2020; 295: 715-21.
[20] Bernheim A, Mei X, Huang M, Yang Y, Fayad ZA, Zhang N, Diao K, Lin B, Zhu X, Li K, Li S, Shan H, Jacobi A and Chung M. Chest CT findings in coronavirus disease-19 (COVID-19): relationship to duration of infection. Radiology 2020; 295: 200463.
[21] Kunhua Li JW, Wu F, Guo D, Chen L, Zheng F and Li C. The clinical and chest CT features associated with severe and critical COVID-19 pneumonia. Invest Radiol 2020; 55: 327-331.
[22] Li S, Liu S, Wang B, Li Q, Zhang H, Zeng L, Ge H, Ma Q and Shen N. Predictive value of chest CT scoring in COVID-19 patients in Wuhan, China: a retrospective cohort study. Respir Med 2020; 176: 106271.
[23] Xu Z, Shi L, Wang Y, Zhang J, Huang L, Zhang C, Liu S, Zhao P, Liu H, Zhu L, Tai Y, Bai C, Gao T, Song J, Xia P, Dong J, Zhao J and Wang FS. Pathological findings of COVID-19 associated with acute respiratory distress syndrome. Lancet Respir Med 2020; 8: 420-2.
[24] Li K, Fang Y, Li W, Pan C, Qin P, Zhong Y, Liu X, Huang M, Liao Y and Li S. CT image visual quantitative evaluation and clinical classification of coronavirus disease (COVID-19). Eur Radiol 2020; 25 1-10.
[25] Huang C, Wang Y, Li X, Ren L, Zhao J, Hu Y, Zhang L, Fan G, Xu J, Gu X, Cheng Z, Yu T, Xia J, Wei Y, Wu W, Xie X, Yin W, Li H, Liu M, Xiao Y, Gao H, Guo L, Xie J, Wang G, Jiang R, Gao Z, Jin Q, Wang J and Cao B. Clinical features of patients infected with 2019 novel coronavirus in Wuhan, China. Lancet 2020; 395: 497-506.
[26] Hansell DM, Bankier AA, MacMahon H, McLoud TC, Muller NL and Remy J. Fleischner Society: glossary of terms for thoracic imaging. Radiology 2008; 246: 697-722.
[27] Wu J, Wu X, Zeng W, Guo D, Fang Z, Chen L, Huang H and Li C. Chest CT findings in patients with corona virus disease 2019 and its relationship with clinical features. Invest Radiol 2020; 55: 257-61.
[28] Wong KT, Antonio GE, Hui DS, Lee N, Yuen EH, Wu A, Leung CB, Rainer TH, Cameron P, Chung SS, Sung JJ and Ahuja AT. Thin-section CT of severe acute respiratory syndrome: evaluation of 73 patients exposed to or with the disease. Radiology 2003; 228: 395-400.
[29] Zhou Z, Guo D, Li C, Fang Z, Chen L, Yang R, Li X and Zeng W. Coronavirus disease 2019: initial chest CT findings. Eur Radiol 2020; 30: 4398-406.
[30] Song F, Shi N, Shan F, Zhang Z, Shen J, Lu H, Ling Y, Jiang Y and Shi Y. Emerging coronavirus 2019-nCoV pneumonia. Radiology 2020; 295: 200274.
[31] Li XY, Zhou Y, Kong ZX, Hou MD, Luo N, Sun WH, Huang N, Yang C, Zhang AD and Li YS. Exploration of CT manifestations of different clinical types of novel coronavirus pneumonia. Ann Palliat Med 2021; 10: 37-44.
[32] Kong W and Agarwal PP. Chest imaging appearance of COVID-19 infection. Radiol Cardiothorac Imaging 2020; 2: e200028.
[33] Pan Y, Guan H, Zhou S, Wang Y, Li Q, Zhu T, Hu Q and Xia L. Initial CT findings and temporal changes in patients with the novel coronavirus pneumonia (2019-nCoV): a study of 63 patients in Wuhan, China. Eur Radiol 2020; 30: 3306-9.